Catal Lett (2007) 118:8–14
DOI 10.1007/s10562-007-9181-y

High Surface Area $CuMn_2O_4$ Prepared by Silica-Aquagel Confined co-precipitation. Characterization and Testing in Steam Reforming of Methanol (SRM)

Gregorio Marbán · Teresa Valdés-Solís · Antonio B. Fuertes

Received: 19 April 2007 / Accepted: 19 June 2007 / Published online: 20 July 2007

Abstract High surface area $CuMn_2O_4$ and mixtures of CuO and Mn_2O_3 were prepared via a novel template technique based on the coagulation—precipitation processes that occur when the metallic cations of salts dissolved in a silica aquagel medium are forced to precipitate by basic reagents. The oxides prepared by this method were tested as catalysts for the methanol steam reforming reaction at 250 °C and a very high space velocity (WHSV = 27.2 h^{-1}). $CuMn_2O_4$ with a high surface area (300 m^2/g) and a tangled structure that apparently resembles the internal surface of the amorphous silica gel was obtained. The catalytic activity of this material is similar to that of the most active catalyst reported in the literature, with the advantage that its stability is enhanced. Contrary to what has been reported for low surface area particles, the physical mixture of copper oxide and manganese oxide nanoparticles prepared by the confined co-precipitation technique displayed a much lower catalytic activity than the spinel.

Keywords Spinel · Template · Precipitation · Methanol steam reforming · Coke deposition · $CuMn_2O_4$

1 Introduction

Copper-based catalysts are known to exhibit high activity towards the production of hydrogen via methanol steam reforming. They have been promoted by several metal oxides such as ZnO [1, 2], CeO_2 [2–4], ZrO_2 [5], or mixtures such as ZnO/ZrO_2 [6] or CeO_2/ZrO_2 [7]. Manganese oxides have also been employed as promoters by Idem and Bakhshi [8, 9] who observed that the presence of $CuMnO_2$ and Mn_2O_3 produced an increase in the catalytic activity of the catalyst. In order to augment the catalytic activity of these structures it is necessary to develop preparation techniques which produce catalysts with a high active surface area. This is the aim of a recently developed nanocasting procedure for the preparation of high surface area inorganic compounds [10, 11], involving the synthesis of these compounds in the nanospaces provided by the pores of a porous solid (hard template), usually silica gel and active carbon [10, 12–14]. Due to the fact that the synthesis takes place in a confined nanospace, sintering of the particles is restricted and the preparation of high-surface area materials is achieved. In a previous work [15] we applied this procedure to the preparation of high surface area catalysts for methanol steam reforming, using silica xerogel as hard template. The best catalytic results were obtained with $CuMn_2O_4$ nanoparticles. In this work we explore a novel approach, called silica aquagel confined co-precipitation (SACOP), for the preparation of high surface area $CuMn_2O_4$ [16]. The key to this novel methodology is that the inorganic precursors are initially mixed with the ingredients used for the synthesis of a silica gel. This circumvents the multiple impregnation steps necessary in the classical hard template routes. Once the silica gel is obtained, the metallic salts are precipitated by adding an appropriate basic agent. In this way, an optimum distribution of inorganic compounds is achieved throughout the silica gel matrix. The calcination of the composite formed (made up of the silica gel and inorganic precipitates) and the subsequent removal of the silica matrix lead to inorganic oxides that have very high surface areas, which are clearly greater than those reported for inorganic

G. Marbán (✉) · T. Valdés-Solís · A. B. Fuertes
Instituto Nacional del Carbón (CSIC), c/Francisco Pintado Fe, 26, Oviedo 33011, Spain
e-mail: greca@incar.csic.es

materials obtained by the classical hard template route. This synthetic method has two additional advantages over the standard hard template routes: (a) inorganic materials with higher yields are obtained and (b) the synthesis of both the inorganic compounds and hard template is based on the use of low-cost reagents (i.e. metal nitrates, sodium silicate and nitric acid).

The goal of this work is to prepare high surface area $CuMn_2O_4$ by the SACOP technique and to test the material in the production of hydrogen by the steam reforming of methanol (SRM).

2 Experimental

2.1 Catalyst Preparation

A $CuMn_2O_4$ nanocatalyst (labeled CuMn-S1, Table 1) was prepared by the silica-aquagel confined co-precipitation method (SACOP), as reported elsewhere [16]. The silica source (sodium silicate, Aldrich, 27% SiO_2 + 14% NaOH) and deionised water were poured under stirring into a Teflon® autoclave. In a different vessel the metallic nitrates were dissolved in a 4 M HNO_3 solution and the resulting mixture was added dropwise to the Teflon® autoclave containing the sodium silicate suspension under stirring. The amounts of each precursor were adjusted in order to establish the following molar compositions in the synthesis suspension: $SiO_2/H^+/H_2O$ = 1/6.54/193.9 and Si/M = 4 (M = total moles of metals in the final metallic oxides). The closed autoclave was left under stirring for 24 h at RT (hydrolysis step), and then placed in an oven at 100 °C for 24 h in order to produce the gel (condensation step). Co-precipitation of the metallic cations confined in the water phase of the resulting gel was carried out with powdered NaOH. In all the precipitations performed it was verified that the final pH was slightly above that needed for precipitating metal hydroxides in water solutions. The slurry formed after the co-precipitation stage was subsequently subjected to several water washing and centrifugation steps, and finally it was dispersed in acetone to replace the remaining water, vacuum filtered and left to dry at RT overnight. The resulting silica-metal hydroxide composites were calcined in air at 550 °C for 4 h. Finally, the silica matrix was removed by dissolution in NaOH (2 M) in an autoclave at ~100 °C over a period of 1–2 days.

In order to check the effect of the preparation conditions on the catalytic activity of the resulting materials, other $CuMn_2O_4$ catalysts were prepared as follows:

(i) CuMn-S2 (Table 1): the metal nitrates were dissolved in the silica aquagel (after the condensation step), instead of being introduced into the precursor solution.

(ii) CuMn-S1-PVI (Table 1): A Mn_2O_3/SiO_2 nanocomposite was prepared by the SACOP technique (with gaseous NH_3 as precipitating agent). After precipitation, a two-step calcination (N_2-400 °C-4 h + Air-800 °C–2 h) was carried out as described by Marbán et al. [17]. Next, the pore volume of the calcined nanocomposite was impregnated with an ethanol solution of copper nitrate, at the same molar ratio as that in $CuMn_2O_4$. The impregnated material was dried at 120 °C and calcined in air at 400 °C for 4 h. Finally, the silica was removed by dissolution in NaOH (2 M).

(iii) Cu + Mn-S1 (Table 1): A Mn_2O_3/SiO_2 nanocomposite was prepared as described in (ii), and the silica was removed by dissolution in NaOH (2 M). CuO was also prepared by SACOP, using powdered NaOH as precipitating agent, by calcining in air at 500 °C for 4 h and removing the silica by dissolution (NaOH, 2 M). The final catalyst was a physical mixture of the Mn_2O_3 and CuO nanoparticles, at a 1:1 molar ratio.

Table 1 Preparation conditions and final SiO_2 contents for the different catalysts

Reference	Prep.	Calcination conditions	SiO_2 (wt%)
CuMn-S1-a	(1)	Air-550 °C-4 h	5.0
CuMn-S1-b	(1)	Air-550 °C-4 h	0.9
CuMn-S2	(2)	Air-550 °C-4 h	4.5
CuMn-S1-PVI	(3)	Mn_2O_3: (N_2-400 °C-4 h) + (Air-800 °C-2 h)	8.9
		CuO + Mn_2O_3: Air-500 °C-4 h	
Cu + Mn-S1	(4)	For CuO: Air-500 °C-4 h	0.0 (Cu) 2.6 (Mn)
		For Mn_2O_3: (N_2-400 °C-4 h) + (Air-800 °C-2 h)	

(1) S1: SACOP with metal precursor addition prior to the hydrolysis step

(2) S2: SACOP with metal precursor addition after gel formation

(3) S1-PVI: S1 for manganese oxide in SiO_2 and further PVI of copper nitrate in ethanol before silica removal

(4) S1 for individual oxides

2.2 Catalyst Characterization

X-Ray Diffraction (XRD) patterns for the oxide particles were obtained in the wide-angle range (2θ = 20–70°) on a Siemens D5000 instrument operating at 40 kV and 20 mA and using Cu Kα radiation (λ = 0.15406 nm). Crystal size values were estimated from the XRD patterns by using the Scherrer equation (d_{XRD}). Nitrogen adsorption isotherms were performed at 77 K on a Micromeritics ASAP 2010 volumetric adsorption system. The BET surface area was deduced from the isotherm analysis in the relative pressure range of 0.04–0.20. Transmission electron microscopy (TEM) was performed in a Jeol Mod. 2000 EX II microscope (200 kV).

The metal distributions and silica contents of the samples were studied by means of a Scanning Electron Microscope (Mod. DSM 942, Zeiss) and an attached Energy Dispersive X Ray Detector (EDX).

2.3 Catalytic Activity and TPR Analysis

Catalytic activity experiments were performed with 20 mg of catalyst diluted in 180 mg of SiC particles (<75 μm) in an electrically heated Vycor reactor (7.1 mm i.d.). The catalyst was pre-treated in helium at 250 °C for 60 min (Flow rate = 200 cm^3/min). Afterwards the reaction was performed at 250 °C in a mixture of 3.51 vol.% CH_3OH and 3.86 vol.% H_2O in He to balance [Flow rate = 200 cm^3/min, WHSV (methanol weight hourly space velocity) = 27.2 h^{-1}]. Methanol and water were injected into the reactor through a vaporizer by a syringe pump. The analysis of products (CH_3OH, H_2O, H_2, CO and CO_2) was performed on-line by mass spectrometry (Omnistar 300O).

As the experiments were carried out under experimental conditions in which water was in excess of methanol and total conversion was relatively low (below 0.4), the effect of water steam, carbon dioxide and hydrogen on the reaction rate can be dismissed and consequently the rate expression can be written as [15]:

$$r_{SRM} = k\, P^{\alpha}_{CH_3OH} \tag{1}$$

Assuming plug flow in the integral reactor, the reaction rate can be evaluated as:

$$r_{SRM} = \frac{F^0_{CH_3OH}}{w_m}\frac{(1-X)^{\alpha}-(1-X)}{1-\alpha} \tag{2}$$

where $F^0_{CH_3OH}$ is the inlet methanol flow (mol/s), w_m is the mass of the catalyst (g), X represents the methanol conversion and r_{SRM} is the reaction rate, expressed in moles of methanol per gram per second.

Finally, the selectivity towards CO_2 formation during the reaction can be evaluated by the following equation:

$$S = \frac{P_{CO_2}}{P_{CO_2}+P_{CO}} \tag{3}$$

where the CO and CO_2 partial pressures are those at the exit of the catalyst bed.

TPR analyses were performed in the same reactor, with 20 mg of catalyst diluted in 180 mg of SiC particles. The sample was heated in helium at 100 °C for 60 min. Afterwards catalyst reduction was performed in 1.7% H_2 in He at a heating rate of 3 °C/min up to 800 °C. H_2 analysis was performed on-line by mass spectrometry (Omnistar 300O).

3 Results and Discussion

3.1 Structural Properties of SACOP Nanocatalysts

As mentioned in a previous paper [16], with the SACOP technique it is possible to prepare metal oxides with values of specific surface area over 100 m^2/g, by employing low cost precursors in a simple synthesis procedure. The sequential steps of the synthesis produce first a dried nanocomposite (metal hydroxides in a silica matrix), then a calcined nanocomposite (metal oxides in a silica matrix) and finally the metal oxide nanoparticles (after silica removal). Figure 1 shows TEM images of the materials obtained after each step during the preparation of CuMn-S1-b. The dried nanocomposite is composed of a silica gel matrix (white grey particles in the images) made up of particles with a wide size distribution, up to ~25 nm, in which small particles (below ~5 nm) of metal hydroxides (dark spots in the figures) seem to be homogeneously embedded. The calcined nanocomposite presents a similar picture, indicating that the calcination step hardly produces any geometrical changes in the structure, this being the main advantage of the technique. After the removal of the silica ($CuMn_2O_4$ images in Fig. 1) the metal oxides exhibit a peculiar structure in the form of thin sheets which seem to be partly unfolded (upper $CuMn_2O_4$ image in Fig. 1) and partly rolled up (lower $CuMn_2O_4$ image in Fig. 1). The thickness of these sheets cannot be directly estimated, although it seems to be below a few nanometers (< 3 nm). This tangled structure appears to resemble the internal surface of the amorphous silica gel, which means that the metal precursors are deposited on the silica gel surface, forming a thin layer during the precipitation step. Therefore, what appear to be small metal hydroxide particles in the TEM images of the dried nanocomposite (Fig. 1) might merely be the result of randomly superimposed metal

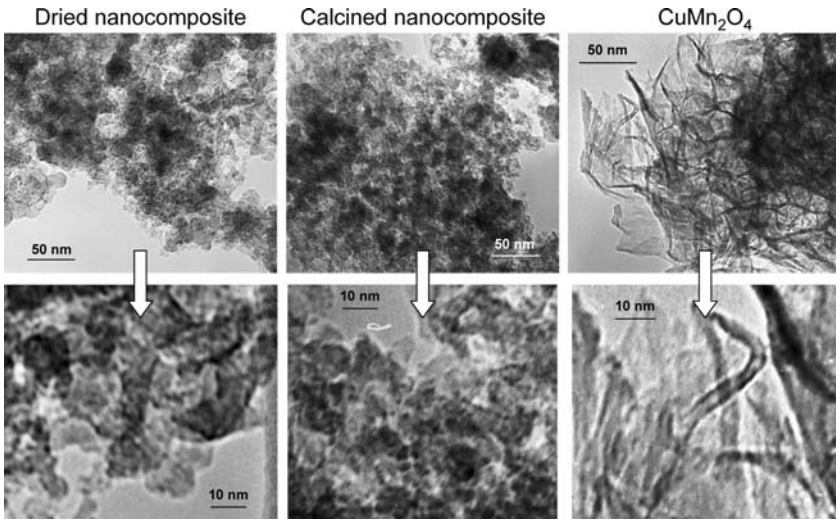

Fig. 1 TEM images, at two different magnification degrees, of the materials obtained at different stages during the preparation of high surface area $CuMn_2O_4$ by SACOP

hydroxide layers, since it is highly unlikely that the metal oxide nanoparticles turn into a continuous sheet during the silica removal step.

As indicated in Table 2, the final oxides in the CuMn-S1 samples (a and b) have slightly different specific surface area values for different residual silica contents. The sample washed for the longest period with the NaOH solution (CuMn-S1-b) has a negligible SiO_2 content and the highest surface area value, almost 300 m^2/g, which means that the residual silica in the CuMn-S1-a (250 m^2/g) is in the form of non-porous but soluble silicates. XRD analyses of the different samples are shown in Fig. 2. The CuMn-S1-b sample exhibits the unequivocal spectrum of $CuMn_2O_4$ (Fig. 1a), with wide peaks that reflect the very small size of the catalyst particles. The application of the Scherrer equation to the main peaks of the spectrum gives a particle size of ~4 nm (d_{XRD}, Table 2), which agrees well with the particle size deduced from the value of the BET surface area, by considering spherical shape of the particles (d_{BET}; Table 2).

The catalysts prepared by varying the technique did not produce the desired hopcalite structure. By adding the metal nitrates to the silica aquagel (CuMn-S2), a mixture of oxides was obtained (Fig. 2). In this sample, the Mn_2O_3 nanoparticles presented a very low particle size of ~4 nm (Table 2), but the CuO particles were considerably larger (~25 nm). The mean pore size of the silica gel, without any metal incorporation, was ~8 nm [16]. This suggests that manganese cations penetrated the porous structure of the silica aquagel, whereas copper cations did not. As a consequence, the BET surface area of the final oxidic sample was somewhat lower (156 m^2/g; Table 2) than that of the samples obtained when the metal nitrates were added to the hydrolysis solution (CuMn-S1 sample). As can be observed in Fig. 2, a similar division of phases was obtained when a Mn_2O_3/SiO_2 nanocomposite prepared by the SACOP technique was pore volume impregnated with an ethanol solution of copper nitrates i.e. a Mn_2O_3 phase with a particle size of around 5 nm and a CuO phase with a particle size of 26 nm (CuMn-S1-PVI sample; Table 2). These results suggest that copper and manganese ions need to associate earlier on during the hydrolysis step to form the hopcalite structure.

Buciuman et al. [18] found that a physical mixture of Mn_2O_3 and CuO particles was more active for CO oxidation than the hopcalite particles. In their work they used catalyst samples produced by the direct evaporation of the metal nitrate solutions in distilled water, followed by cal-

Table 2 Values of particle size and specific surface area for the different catalysts

Catalyst	d_{XRD} (nm)			S_{BET} (m^2/g)/d_{BET} (nm)		
	CuO	Mn_2O_3	$CuMn_2O_4$	CuO	Mn_2O_3	$CuMn_2O_4$
CuMn-S1-a			4			250/4.4
CuMn-S1-b			4			296/3.7
CuMn-S2	25	3.8		← 156/7.0 →		
CuMn-S1-PVI	26	4.9		← 177/6.2 →		
Cu + Mn-S1	8.3	4.4		104/9.0	240/5.6	

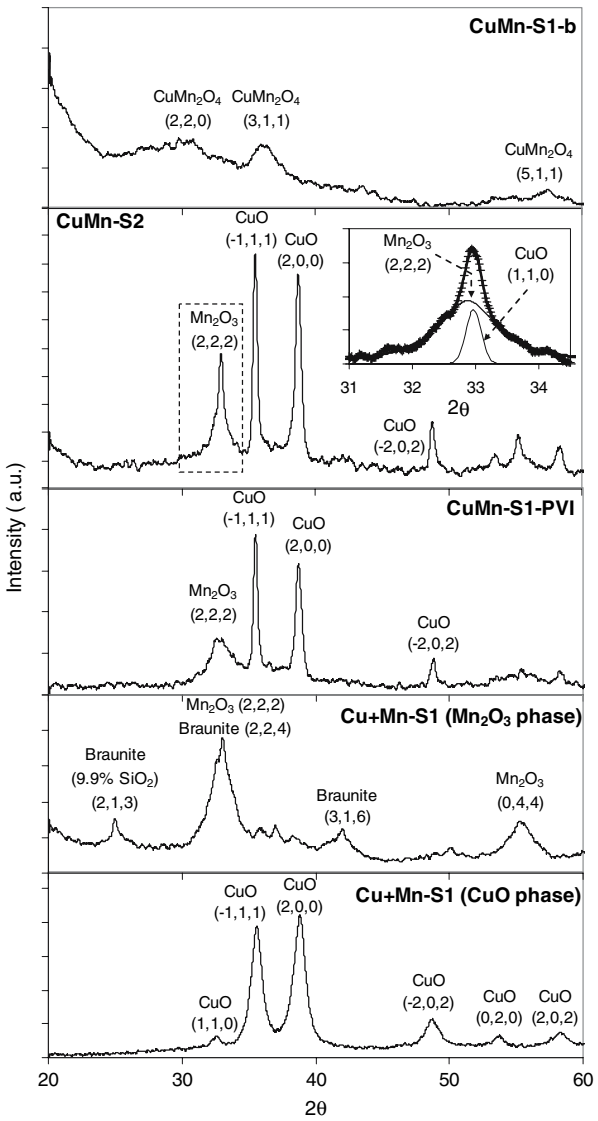

Fig. 2 XRD analyses of the materials prepared in this work

cination. Their samples, therefore, displayed very low values of surface area (below 3 m^2/g). To assess whether the better catalytic activity of the physical mixture of oxides could be achieved when dealing with nanoparticles in the SRM, Mn_2O_3 and CuO nanoparticles were prepared by the SACOP technique, as explained in the experimental section. Figure 2 shows the XRD spectra for both samples: CuO was obtained in a pure state (0 wt% SiO_2; Table 1) with an XRD particle size of a little over 8 nm, close to that evaluated from the BET analysis (~9 nm, 104 m^2/g; Table 2). The Mn_2O_3 particles obtained exhibited a small SiO_2 content (2.6 wt%; Table 1) which must be ascribed to the presence of a low proportion of silicates (braunite) in the final sample, as detected by XRD (Fig. 2). The XRD size of the Mn_2O_3 particles was, as expected, quite low (~4 nm; Table 2).

3.2 TPR Analyses

Figure 3 shows the TPR results obtained for the different samples. In all cases the estimated overall degrees of reduction (depending on each case, from $CuMn_2O_4$ to Cu + MnO, from CuO to Cu or from Mn_2O_3 to MnO) were about 80% of the theoretical maximum reduction degrees (exact values indicated in Fig. 3). The moisture content and a slightly reduced state of the initially weighted samples might explain why a 100% reduction degree was not achieved. The profiles can be compared to those obtained by Buciuman et al. [18] for low-surface area samples

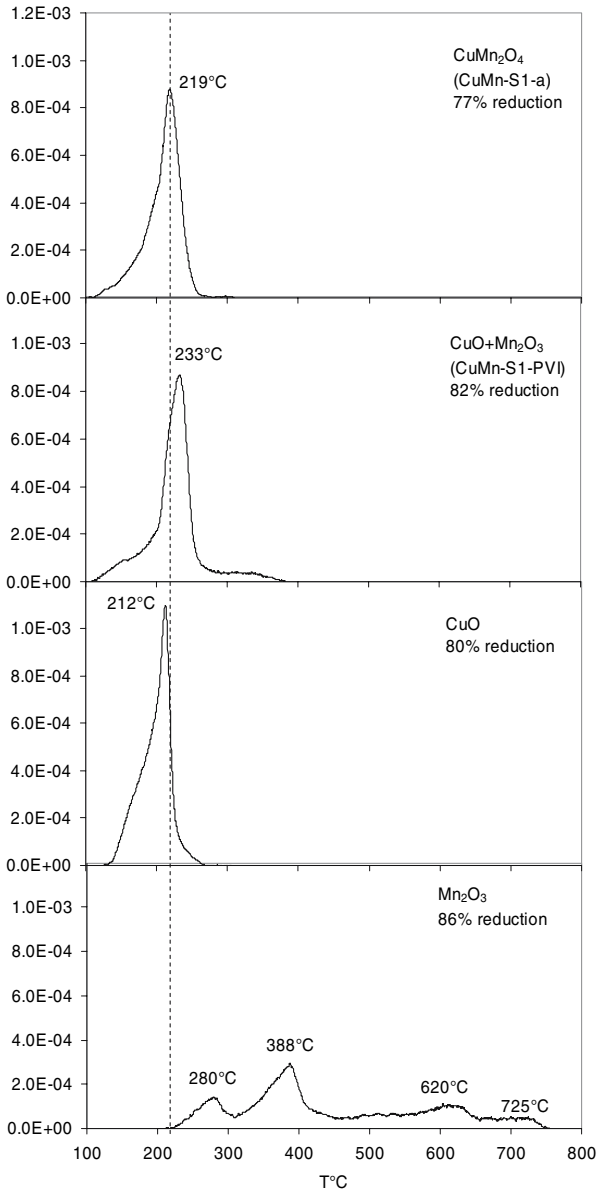

Fig. 3 TPR profiles of the materials prepared in this work. TPR profiles of CuO and Mn_2O_3 correspond to the single oxides prepared by SACOP prior to their physical mixture to form Cu + Mn-S1

(<3 m^2/g). In general, the shapes of the profiles are very similar though the peaks are clearly displaced towards lower temperatures for the nanoparticulate samples. Thus, the characteristic peak temperatures are 219 °C for CuMn-S1-a (320 °C for the equivalent low-surface area sample in the work of Buciuman et al. [18]), 212 °C for CuO (330 °C in [18]) and 280 and 388 °C for Mn_2O_3 (445 and 525 °C in [18]). In the latter sample these two peaks represent the consecutive reduction steps $Mn_2O_3 \rightarrow Mn_3O_4 \rightarrow MnO$ [19], whereas the high temperature peaks (620 and 725 °C) that complete the profile (Fig. 3) correspond to the reduction of the braunite silicate detected by XRD. It should be noted that the spinel sample (CuMn-S1-a in Fig. 3) exhibits a reduction peak similar to that of CuO, and that no H_2 consumption peaks are observed at the temperatures typical of manganese oxides. A similar low-temperature peak is observed in the case of CuMn-S1-PVI, where CuO and Mn_2O_3 are detected by XRD. This indicates that the presence of copper compounds enhances the reducibility of manganese phases (lower temperatures are needed to reduce them) even if the spinel is not formed, while the reducibility of copper phases hardly changes. In general, the nanoparticulate systems show TPR profile displacements towards lower temperatures with respect to the low-surface area particles [18], in the range of 100–150 °C. This high reducibility of the nanoparticulate system, which is obviously linked to the high dispersion of the species involved, is in direct relation with the higher activity expected for the SRM reaction [20].

3.3 Catalytic Activity

Figure 4 shows the variation in catalytic activity and selectivity at 250 °C with time on stream (T.O.S.) for the catalysts prepared in this work. The spinel CuMn-S1-b is clearly superior to the other catalysts, both in terms of activity and selectivity. Catalysts prepared by the addition of metal nitrates in the silica aquagel (CuMn-S2) or by pore volume impregnation of the Mn_2O_3/SiO_2 nanocomposite (CuMn-S1-PVI) display almost identical catalytic properties. This is a reasonable result considering the structural similarities of both catalysts (Fig. 2 and Table 2). The lower catalytic activity with respect to the spinel catalyst must be ascribed to a less intimate contact between the copper and manganese phases and a lower active surface area (Table 2). The worst catalytic result was obtained for the physical mixture of CuO and Mn_2O_3 nanoparticles (Cu + Mn-S1 in Fig. 4), even though both phases present optimal textural properties. It seems evident that the spinel structure favours the reaction, possibly through the enhanced mobility of lattice oxygen between the copper and manganese phases. It should be noted, however, that all the catalysts prepared in this work have comparable or higher catalytic activities than those of many previous catalysts reported in the literature. This can be checked by a comparison of the reaction rates, as determined by equation (2), which is available in [15]. The catalytic properties of the best catalyst prepared in this work (CuMn-S1-b) and the most active non-noble metal-based catalyst reported in [15] are compared in Table 3. As can be seen, the initial catalytic activity values of both materials are similar,

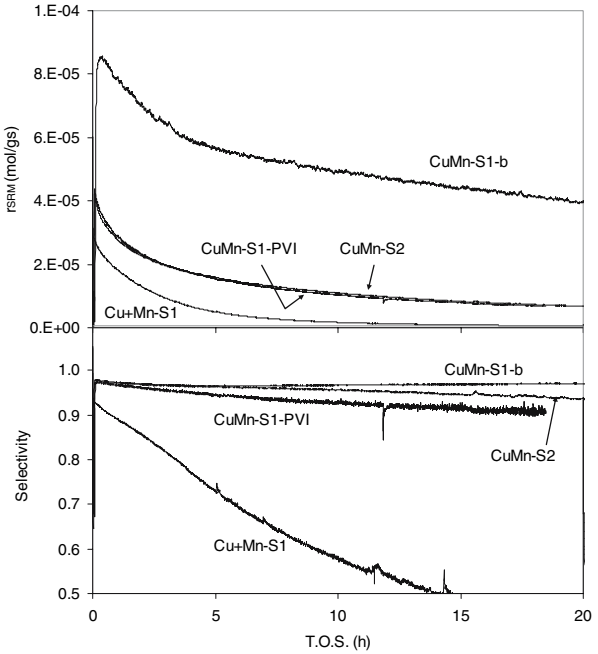

Fig. 4 Reaction rates (α = 0.65) and selectivity values at 250 °C for the materials prepared in this work and tested in the SRM reaction

Table 3 Comparison of the best catalyst obtained in this work with the best catalyst obtained in [15]

Catalyst	T (°C)	WHSV (h^{-1})	$P^0_{CH_3OH}$ (Pa)	TOS (h)	r_{SRM} ($\times 10^5$ mol/(sg))		Selectivity
					α = 0.27	α = 0.65	
S-CuMn-b [15]	250	51.6	7120	1	8.1	7.8	0.98
				20	2.4	2.4	0.95
CuMn-S1-b (this work)	250	27.2	3554	1	8.7	7.9	0.97
				20	4.2	4.0	0.97

though the catalyst prepared in the present work is considerably more stable, with almost double the activity and a better selectivity at 20 h on stream. This enhanced stability might be ascribed to a lower spatial velocity (27.2 vs 51.6 h^{-1}) or a lower methanol inlet partial pressure (3500 vs 7000 Pa), which may alter the equilibrium of unwanted side reactions such as coke deposition. A bit higher stability is commonly reported for the few catalysts described in literature which were submitted to stability tests. Following the above reasoning, this could be due to the low values of spatial velocities used in most works (i.e. 2.6 [2], 3.3 [21], 3.9 [22], 11.7 [23], 24.4 [6] h^{-1}), as compared to those used in testing our catalysts (WHSV = 27–52 h^{-1}). In fact, some of these literature catalysts [6, 21] were prepared in our lab and tested at high WHSV (52 h^{-1}), showing a much faster deactivation rate [15] and thus corroborating this assumption.

4 Conclusions

The silica aquagel confined precipitation (SACOP) technique has proven to be a valuable instrument for the preparation of active nanocatalysts for the SRM. $CuMn_2O_4$ obtained by SACOP has a surface area of 300 m^2/g and a particle size of ~4 nm. The catalytic activity of this material for the SRM reaction is among the highest ever reported in the literature. Other catalysts prepared by varying this technique, such as chemical or physical mixtures of CuO and Mn_2O_3, displayed much lower degrees of catalytic activity.

Acknowledgments Funding by the Spanish National Project MAT2005-00262 and the FICYT Regional Project (IB05-001) is acknowledged. TVS thanks the CSIC-ESF for the award of a post-doctoral I3P contract.

Reference

Choi Y, Stenger HG (2002) Appl Catal B: Environ 38:259–269
Liu Y, Hayakawa T, Tsunoda T, Suzuki K, Hamakawa S, Murata K, Shiozaki R, Ishii T, Kumagai M (2003) Top Catal 22:205–213
Papavasiliou J, Avgouropoulos G, Ioannides T (2004) Cat Comm 5:231–235
Liu Y, Hayakawa T, Suzuki K, Hamakawa S, Tsunoda T, Ishii T, Kumagai M (2002) Appl Catal A Gen 223:137–145
Purnama H, Girgsdies F, Ressler T, Schattka JH, Caruso RA, Schomäcker R, Schlogl R (2004) Cat Lett 94:61–68
Matter PH, Braden DJ, Ozkan US (2004) J Catal 223:340–351
Oguchi H, Nishiguchi T, Matsumoto T, Kanai H, Utani K, Matsumura Y, Imamura S (2005) Appl Catal A Gen 281:69–73
Idem RO, Bakhshi NN (1995) Ind Eng Chem Res 34:1548–1557
Idem RO, Bakhshi NN (1996) Chem Eng Sci 51:3697–3708
Fuertes AB (2005) J Phys Chem Sol 66:741–747
Valdés-Solís T, Marbán G, Fuertes AB (2005) Chem Mater 17:1919–1922
Schüth F (2003) Angew Chem Int Ed 42:3604–3622
Valdés-Solís T, Fuertes AB (2006) Mater Res Bull 41:2187–2197
Schwickardi M, Johann T, Schmidt W, Schüth F (2002) Chem Mater 14:3913–3919
Valdés-Solís T, Marbán G, Fuertes AB (2006) Catal Today 116:354–360
Marbán G, Valdés-Solís T, Fuertes AB (2007) Microp Mesop Mat submitted
Marbán G, Valdés-Solís T, Fuertes AB (2004) Phys Chem Chem Phys 6:453–464
Buciuman FC, Patcas F, Hahn T (1999) Chem Eng Proc 38:563–569
Kapteijn F, Singoredjo L, Andreini A, Moulijn JA (1994) Appl Catal B: Environ 3:173–189
Lindstrom B, Pettersson LJ, Menon PG (2002) Appl Catal A-Gen 234:111–125
Zhang XR, Shi P, Zhao J, Zhao M, Liu C (2003) Fuel Proc Tech 83:183–192
Shishido T, Yamamoto Y, Morioka H, Takaki K, Takehira K (2004) App Catal A-Gen 263:249–253
Cheng WH, Chen I, Liou JS, Lin SS (2003) Top Catal 22:225–233